Neuropsychologia 158 (2021) 107893

Contents lists available at ScienceDirect

Neuropsychologia

journal homepage: www.elsevier.com/locate/neuropsychologia

Representation of semantic typicality in brain activation in healthy adults and individuals with aphasia: A multi-voxel pattern analysis

Ran Li *, Tyler K. Perrachione, Jason A. Tourville, Swathi Kiran

Department of Speech, Language & Hearing Sciences, Boston University, Boston, MA, USA

ARTICLE INFO

Keywords:
Aphasia
Semantic processing
Typicality
fMRI
Multi-voxel pattern analysis

ABSTRACT

This study aimed to investigate brain regions that show different activation patterns between semantically typical and atypical items in both healthy adults and individuals with aphasia (PWA). Eighteen neurologically healthy adults and twenty-one PWA participated in an fMRI semantic feature verification task that included typical and atypical stimuli from five different semantic categories. A whole-brain searchlight multi-voxel pattern analysis (MVPA) was conducted to classify brain activation patterns between typical and atypical conditions in each participant group separately. Behavioral responses were faster and more accurate for typical vs. atypical items across both groups. The searchlight MVPA identified two significant clusters in healthy adults: left middle occipital gyrus and right calcarine cortex, but no significant clusters were found in PWA. A follow-up analysis in PWA revealed a significant association between neural classification of semantic typicality in the left middle occipital gyrus and reaction times in the fMRI task. When the typicality effect was examined for each semantic category at the univariate level, significance was identified in the visual cortex for *fruits* in both groups of participants. These findings suggest that semantic typicality was modulated in the visual cortex in healthy individuals, but to a lesser extent in the same region in PWA.

1. Introduction

The neural representation of conceptual and semantic knowledge in the human cortex has been widely studied in both healthy adults and persons with aphasia (PWA). Category representation is thought to be determined by the internal structure of object categories, including among other factors, *semantic typicality*. Psycholinguistic evidence in both healthy individuals and PWA suggests differential responses for typical and atypical exemplars. However, the neural mechanisms for the typicality effect have not been well established. Distinct neural patterns of representation for typical versus atypical exemplars that follow the behavioral differences would further our understanding of how categories and their specific examples are represented in the brain. The present study examined brain regions that show neural encoding of semantic typicality in both healthy adults and PWA using a multi-voxel pattern analysis (MVPA), which allowed for the detection of brain activation patterns across multiple voxels relative to traditional fMRI approaches that measure only magnitude of activation (Kriegeskorte et al., 2006). The rest of the introduction discusses the current evidence of behavioral and neural responses to typicality in healthy individuals and PWA.

1.1. Behavioral correlates of semantic typicality

It is well known that category structure and representation are determined by several factors such as frequency, familiarity, animacy etc. (Boster, 1988; Malt and Smith, 1982). Of these, exemplar typicality is another organizing principle of the internal structure of semantic categories. Previous psycholinguistic studies in healthy adults have examined the typicality effect using a variety of experimental paradigms, such as category membership verification (Hampton, 1979; Larochelle and Pineau, 1994), ratings of typicality of items in a category (Rosch, 1975; Rosch and Mervis, 1975), the order in which category items are learned (Rosch and Mervis, 1975), and category naming frequency (Hampton, 1995). These studies have all identified a robust typicality effect, as evidenced by shorter reaction times, faster learning, and/or more accurate responses for typical than atypical items.

Different theoretical accounts have been proposed to explain the typicality effect. According to the prototype, or *family resemblance hypothesis* models (Rosch and Mervis, 1975), categories are represented by

* Corresponding author. Department of Speech, Language & Hearing Sciences, 635 Commonwealth Ave, Boston University, Boston, MA, 02215, USA.
E-mail address: rli92@bu.edu (R. Li).

https://doi.org/10.1016/j.neuropsychologia.2021.107893
Received 24 September 2020; Received in revised form 31 March 2021; Accepted 13 May 2021
Available online 19 May 2021
0028-3932/Published by Elsevier Ltd.

a set of features that may carry more or less weight in the prototype (e.g., *birds: robin*), which is the summary description of all category members based on features. This theory postulates that typicality is determined by the extent to which features are shared between the prototype and category members. Typical members of a category are more similar to the prototype as they share more semantic features with the prototype, whereas atypical members are less similar to the prototype as they share fewer features with the prototype. The semantic complexity hierarchy further suggests that atypical items have a more complex representation, as they carry a wider range of semantic features including core (e.g., *birds: has wings*), distinctive (e.g., *runs, long legs*), and prototypical (e.g., *flies*) features, whereas typical items are easier to access because they comprise only core and prototypical features (Kiran, 2007).

An alternative perspective of typicality is the exemplar theory, which assumes that the summary description of the category (i.e., prototype) is not needed. In this account, categories are represented in memory by actual exemplars that have previously been encountered and are labeled with their category name (Nosofsky and Palmeri, 1997; Nosofsky and Zaki, 2002). With continued learning experience, memories for these exemplars are eventually formed and used for categorization or recognition of stimuli (Nosofsky and Zaki, 2002; Rouder and Ratcliff, 2006). According to this exemplar-based model, typicality is conceptualized as the summed similarity of a category member to all the stored members of that category (Nosofsky, 1988). Hence, typical items are accessed faster and more accurately as they are more similar to the stored exemplars, whereas atypical items are accessed slower and less accurately because they are less similar to the stored exemplars (Nosofsky, 1988).

The same behavioral typicality effect has even been reported in PWA (Kiran et al., 2007; Kiran and Thompson, 2003; Sandberg et al., 2012). For example, one study examined the effect of typicality on online category verification of inanimate categories in normal young, normal older, and aphasic patients with and without semantic impairment (Kiran et al., 2007). Participants were asked to decide if the target word that was either a typical, atypical, or nonmember of a category belonged to the preceding category label. Results showed that even though PWA performed worse on the task than healthy individuals, their responses to typical items were faster and more accurate than atypical items, a pattern similar to healthy controls.

In contrast, the typicality effect was not found in other studies including PWA (Rogers et al., 2015; Sandberg et al., 2012). For example, Sandberg et al. (2012) examined the effect of semantic typicality in healthy controls and PWA for categories that varied in terms of category boundaries and gradedness using the online category verification paradigm. The results showed a consistent typicality effect in healthy controls across tasks, but a reduced effect in some PWA specific to the severity of semantic impairment. Rogers et al. (2015) further examined the effect of typicality on a variety of language tasks in patients with semantic dementia (SD; bilateral anterior temporal lobe/ATL atrophy) whose semantic representations are distorted, and patients with semantic aphasia (SA; left fronto-parietal and/or posterior temporal stroke) whose semantic control may be affected. In the SA group, typicality effect was identified in two tasks: 1) picture sorting, in which accuracy was higher for sorting typical than atypical items into specific categories, and 2) word-picture matching, in which accuracy was lower for typical items when picture distractors were close, and accuracy was lower for atypical items when distractors were distal. However, the typicality effect was not significant in the picture naming task. The authors explained these findings within the context of the controlled semantic cognition (CSC) model, which provides a joint account of semantic representation and control (Lambon Ralph et al., 2016). The CSC model suggests that semantic representations are mediated by a single hub situated in the bilateral ATLs (Patterson et al., 2007), and a fronto-temporoparietal control system in the posterior middle temporal gyrus (pMTG), the prefrontal cortex (PFC), and the intraparietal sulcus (IPS), that is involved to manipulate activation in the network for semantic representations. In individuals with SA, the semantic impairment stems from damage to the control system that shapes the flow of activation through the hub-and-spokes network, leading to noisy processing within the semantic network as the balance of activation and inhibition is disrupted. Thus, since typical items are more similar to other category members than atypical items, a larger degree of semantic control is required to resolve the semantic competition elicited by the typical items, resulting in reduced typicality effect in individuals with SA.

1.2. Neural correlates of semantic typicality

Even though the behavioral typicality effects are fairly robust in healthy individuals and to a certain extent in PWA, whether these differences in category exemplar representation are instantiated in the brain is not completely clear. Two neuroimaging studies to date have utilized fMRI to examine the neural representation of typicality in healthy individuals. One study compared neural response patterns of the most and least typical items in each category to the category central tendency (i.e., the average neural patterns of all exemplars in a category) in healthy young adults (Iordan et al., 2016). Participants were exposed to picture stimuli of different semantic categories and were asked to perform an fMRI one-back repetition task. A region of interest (ROI) MVPA showed that neural response patterns to typical exemplars were more similar to the central category tendency than less typical exemplars in the lateral occipital complex (LOC), suggesting that the LOC plays an important role in the processing of typicality. Another fMRI study investigated the neural representation of typicality via the implementation of an artificial categorization task (Davis and Poldrack, 2014). The results showed that neural typicality, that is, similarity of brain activation patterns between category members and the central tendency, was significantly correlated with participants' perceptions of typicality in early visual regions and regions of the right temporal fusiform and medial temporal lobes. These results suggest that the processing of typical and atypical exemplars may engage visual and temporal regions in healthy individuals. Specifically, visual regions are likely associated with processing the attributes and semantics of category members (Martin et al., 1996; Tyler et al., 2003), and the temporal lobe is involved in semantic processing that integrates visual information for conceptual retrieval (Binder et al., 2009).

In general, the findings from these two studies are consistent with neural models of semantic processing, including the left-lateralized network of frontal, parietal, temporal and prefrontal regions that is involved in a high level of integration in receiving, storing, and processing semantics (Binder et al., 2009, 2011). The activations identified in the temporal and/or temporo-occipital regions suggest that typicality may involve both visual and semantic processing. More specifically, these results also align with the distributed model of category representation (Tyler et al., 2000), which has primarily focused on explaining category specific impairments after brain damage (i.e., disproportionate difficulty with specific categories; Hillis and Caramazza, 1991; Gainotti, 2000). This model suggests that object concepts vary in the number and types of attributes, the degree to which these attributes are shared or distinctive, and the strength of the relationships between these attributes. Therefore, concepts with shared features may be more resistant to brain damage as these features are intercorrelated and reinforce each other with mutual activation (Tyler and Moss, 1998; Tyler et al., 2003). This model also posits that categories are represented through a distributed but partially overlapping network involving the frontal, temporal, parietal, and occipital lobes. Hence, activations in the temporal and visual regions for typicality processing suggest that categories are represented by the internal structure in these brain regions.

To our knowledge there are no neuroimaging studies examining the effects of typicality in PWA. As mentioned earlier, the behavioral typicality effect in PWA was identified in some studies but not all. Since semantic aphasia is often associated with damage to the left prefrontal and/or temporo-parietal regions, we would expect that damage to the traditional language network would affect the processing of typicality in

PWA due to impaired semantic representations. If the neural correlates of typicality are located in visual regions (Davis and Poldrack, 2014; Iordan et al., 2016), then the typicality effect in PWA would be identified in the same regions as long as they are spared from damage. If typicality involves semantic processing in temporal regions, the typicality effect would also be identified in these regions of PWA. These predictions can be potentially resolved by examining differential patterns of activation associated with behavioral differences between typical and atypical examples in PWA who present with damage to the fronto-temporal network, thereby providing insights into how semantic categories and the internal structure are represented in the damaged brain.

1.3. The current study

The overarching goal of the current study was to examine the processing of typical and atypical exemplars in both healthy individuals and PWA, in order to understand how semantic typicality is organized in both healthy and damaged brains through the following research questions:

Question 1: Which brain regions show distinguishable neural response patterns associated with behavioral responses between typical and atypical items in healthy adults?

Hypotheses 1: According to previous behavioral studies (Rosch et al., 1976; Hampton, 1995), healthy individuals would show a significant typicality effect. Specifically, behavioral responses to typical exemplars would be faster and more accurate than atypical exemplars. According to previous fMRI studies in healthy individuals (Davis and Poldrack, 2014; Iordan et al., 2016), we expected to identify a typicality effect in visual and temporal regions.

Question 2: Which brain regions show distinguishable neural response patterns associated with behavioral responses between typical and atypical items in PWA?

Hypothesis 2: According to previous behavioral studies examining semantic typicality in PWA (Kiran and Thompson, 2003; Kiran et al., 2007; Rogers et al., 2015), responses in patients would be slower and less accurate than in healthy adults, but the behavioral typicality effect would exist, i.e., responses to typical items would be faster and more accurate than atypical items. Our primary prediction was the neural activation patterns consistent with a behavioral typicality effect would most likely be identified in visual regions (Iordan et al., 2016) if they were spared from damage. Secondly, if the processing of typical and atypical exemplars involved semantic representations, the temporal cortex may also be identified through the MVPA. However, since the patients with aphasia were likely to present with varying degrees of damage to the temporal lobe, this prediction was dampened due a possible lack of power in detecting change.

In this study, a pattern-based MVPA was conducted to address these research questions. MVPA is one way of detecting neural correlates of typicality in fMRI data. It allows for the capture of neural information across multiple voxels relative to the traditional fMRI univariate analysis, which does not consider the spatial distribution of information (Mahmoudi et al., 2012). Further, a whole-brain searchlight MVPA is commonly used to analyze human fMRI data (Kriegeskorte et al., 2006) when there are extremely high dimensional brain voxels and a small number of samples as in the present study, which is likely to cause the "curse-of-dimensionality" problem. This approach has additional benefits in that it does not require *a priori* region specification, and it does not cause computational difficulties when there are more voxels than examples (Etzel et al., 2013). For all of these reasons, a whole-brain searchlight MVPA approach was applied to the data in this study to examine neural correlates of semantic typicality.

2. Methods

2.1. Subjects

This study was conducted on a retrospective dataset that initially included N = 35 individuals with chronic aphasia (10 female, 25 male; mean age = 61.54 ± 10.97 years, mean time post onset = 60.43 ± 85.37 months) due to a single left hemisphere stroke, and N = 21 neurologically healthy individuals (11 female, 10 male; mean age = 59.61 ± 13.13 years) who completed scanning for the *Center for the Neurobiology of Language Recovery (CNLR)* conducted at Boston University. Of the initial sample, three healthy individuals and one patient were excluded due to poor fMRI data acquisition. In addition, 13 patients (3 female, 10 male) with lesions extending to the visual cortex were excluded as we attempted to examine activation patterns consistent with healthy adults (Iordan et al., 2016). An attempt to exclude patients based on temporal lobe damage failed because all 35 patients had lesion damage in the temporal cortex, as shown in the lesion overlay (Fig. 1). This process resulted in a final sample including N = 18 healthy individuals (8 female, 10 male; mean age = 59.86 ± 10.50 years) and N = 21 PWA (Table 1; 7 female, 14 male; mean age = 60.71 ± 10.65 years, mean time post onset = 65.43 ± 102.25 months). Exclusion criteria included other psychiatric or neurological disorders other than stroke, and incompatibility with MRI. All participants but three PWA were right-handed. All participants exhibited normal or corrected-to-normal visual and hearing, and reported English as their primary language. Written informed consent was obtained in accordance with the Boston University Institutional Review Board (IRB) protocol.

2.2. Standardized language assessments

Prior to scanning, PWA completed standardized assessments to examine their linguistic and cognitive abilities (Table 1). Tests administered included the Western Aphasia Battery-Revised (WAB-R; Kertesz, 2007) to measure overall aphasia severity (range: 11.7–95.2); the Boston Naming Test (BNT; Kaplan et al., 2001) to measure naming abilities (range: 0–54); the Pyramids and Palm Trees (PPT; Howard and Patterson, 1992) to examine nonverbal semantic association abilities (range: 34–51), and subtest 51: Word Semantic Association from the Psycholinguistic Assessment of Language Processing in Aphasia (PALPA; Kay et al., 1996) to assess lexical-semantic association skills (range: 3–26). Most patients had semantic impairment according to Table 1 and performance varied by overall aphasia severity.

2.3. Stimuli

Stimuli included color photographs of real items from three natural semantic categories (*birds, vegetables, fruits*) and two man-made categories (*furniture, clothing*). Pictures corresponded to concrete nouns that were balanced for familiarity, length, lexical frequency (CELEX; Van der Wouden, 1990) and concreteness (Coltheart, 1981). The stimuli were derived from a previous experimental task that collected semantic typicality ratings of multiple items from nearly 500 individuals (not enrolled in the present study) using MTurk (Meier et al., 2016). That task asked participants to either rate each item using a 1–5 scale (1 = most typical, 5 = most atypical) or define as a non-category member. A list was created with only the items receiving ratings from at least 20 individuals and their typicality values reflected the average rating across participants tested on those items. Items were organized from most to least typical and 18 items from the top and 18 from the bottom of the list were selected as typical and atypical exemplars for each semantic category as stimuli (see Table 2 for the average typicality rating by category, and Appendix A for a sample of task stimuli). Two-sample t-tests showed significant difference between typical and atypical conditions across all items ($p < 0.05$) as well as within each category ($ps < 0.05$). An additional set of 36 items consisting of pixelated scrambled

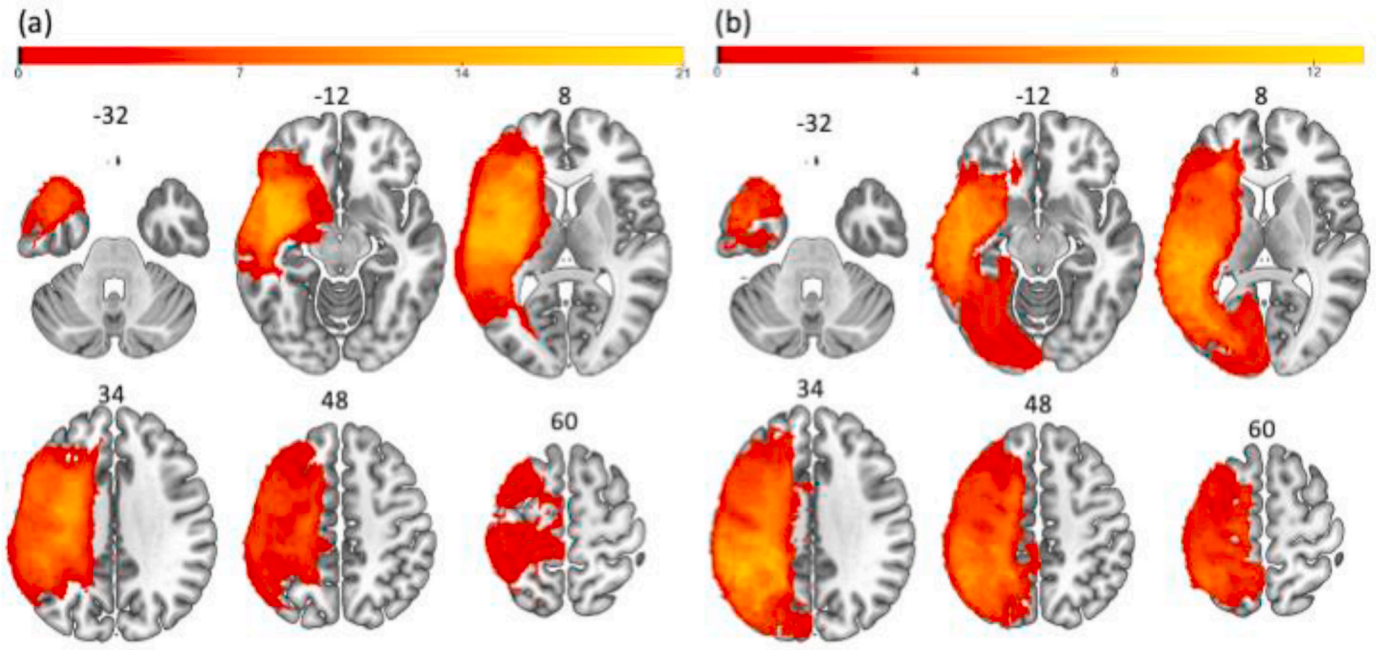

Fig. 1. Overlay of lesion masks. (a): lesion overlay across PWA included ($n = 21$) in the current study; (b): lesion overlay across PWA excluded ($n = 13$) from this study. Color bar indicates the number of patients with overlapping lesion. Images are displayed in neurological convention (left on left). (For interpretation of the references to color in this figure legend, the reader is referred to the Web version of this article.)

Table 1
Patient demographics and standardized assessment data.

ID	Sex	Age (years)	MPO	Aphasia Type	Lesion Volume (mm^3)	WAB-R AQ	PPT	PALPA 51	BNT
PWA11	M	65	16	Broca	247,593	11.7	43	10	0
PWA10	F	48	14	Broca	164,327	13	40	10	0
PWA1	F	50	29	Global	57,246	25.2	49	3	1
PWA9	M	80	22	Broca	89,026	28.9	43	8	1
PWA13	F	76	33	Broca	184,390	37.5	34	19	2
PWA4	M	68	104	Broca	186,845	40	46	12	1
PWA12	M	60	24	Wernicke	172,812	45.2	42	6	6
PWA16	M	62	15	Broca	76,654	56	51	15	21
PWA14	F	64	115	Broca	127,704	58	36	12	15
PWA17	M	58	23	Broca	186,520	61.8	51	18	10
PWA6	F	64	24	Broca	96,932	64.4	49	16	41
PWA7	M	61	152	Anomic	163,488	74.3	51	21	54
PWA8	F	70	152	Anomic	69,643	78	50	15	24
PWA20	M	68	21	Anomic	80,283	78.6	49	16	31
PWA2	M	49	52	Anomic	87,587	82.8	48	22	51
PWA15	M	65	17	Anomic	34,148	84.3	50	21	41
PWA18	M	39	18	Anomic	26,221	90.1	51	14	36
PWA21	M	53	467	Anomic	120,817	91.2	49	22	51
PWA19	M	62	21	Anomic	1,565	92	49	21	39
PWA5	M	42	18	Anomic	12,131	92.7	49	21	43
PWA3	F	71	37	Anomic	11,660	95.2	50	26	45
Mean		60.76	65.71		104,647	61.95	46.67	15.62	24.43
SD		10.64	102.13		69,682.17	27.39	5	6.02	19.98

The assessment scores (WAB-R AQ, PPT, PALPA 51, and BNT) are color-coded based on the severity (lower scores are in red). Patients with lower AQ scores appear on the top in this table. PWA: patients with aphasia; MPO: months post onset; WAB-R AQ: Western Aphasia Battery-Revised Aphasia Quotient (max score = 100); PPT: Pyramids and Palm Trees (max score = 52); PALPA 51: Psycholinguistic Assessment of Language Processing in Aphasia Word Semantic Association (max score = 30); BNT: Boston Naming Test (max score = 60); F: Female; M: Male; SD: standard deviation.

pictures of the experimental stimuli served as control items.

Semantic features were also validated using a previous MTurk study (Sandberg et al., 2020) and were used to derive stimuli in the current fMRI task. The MTurk participants (not enrolled in the present study) were shown exemplar pictures and were asked to indicate whether a semantic feature applied to a specific item by providing a "Yes" or "No" response. Defining type (features shared by more than 80% of the items in the category), characteristic type (features shared by less than 80% of the items within the category), unrelated features (features that applied to some category members but not the target item), and non-category features (features that do not apply to any category members) were assigned as applicable or not applicable to target items based on response average. In the current fMRI task, semantic features were controlled for type of information conveyed such as number of physical, functional, and contextual features, as well as whether they were defining or characteristic of the category (see Appendix B for a sample of semantic features).

2.4. fMRI task

During the fMRI task, each participant was assigned three categories of stimuli, including *fruits* plus two other categories that were pseudo-randomly counterbalanced across participants.[1] Experimental and control trials were randomized and presented across two separate runs. Each run consisted of 27 typical and 27 atypical trials across three categories (i.e., 9 trials per typicality per category) and 18 control trials per run. During fMRI scanning, participants performed a semantic feature verification task on the stimuli. The task employed an event-related design with randomized inter-stimulus intervals (ISIs) between 2 and 4 s (Bandettini and Cox, 2000) and was implemented using E-Prime 2.0 (Schneider et al., 2002). Each experimental trial presented a picture together with a written semantic feature below for 5 s (Fig. 2). Next, a fixation cross appeared on the screen during the 2–4 s ISI, and participants were instructed to answer "Yes" or "No" to whether the presented semantic feature applied to the picture by button press. On control trials, participants were presented with a scrambled picture and were required to determine color judgement (i.e., *black and white, color*) using the same

[1] Fruits were assigned to all participants as it was used as the monitored items for a subsequent language treatment for PWA. Details of the treatment can be found in Gilmore et al. (2020).

Table 2
Average typicality ratings by category used in the fMRI semantic verification task.

		Birds	Vegetables	Clothing	Furniture	Fruits
All items	Mean ± SD	2.16 ± 0.69	2.52 ± 1.04	2.60 ± 1.08	3.44 ± 1.70	2.54 ± 0.98
	Range	1.12–3.71	1.00–4.76	1.06–4.95	1.00–5.93	1.00–4.14
Typical items	Mean ± SD	1.59 ± 0.32	1.63 ± 0.35	1.66 ± 0.46	1.97 ± 0.95	1.65 ± 0.44
	Range	1.12–2.06	1.00–2.24	1.06–2.47	1.00–3.60	1.00–2.34
Atypical items	Mean ± SD	2.73 ± 0.44	3.41 ± 0.66	3.53 ± 0.60	4.91 ± 0.70	3.42 ± 0.35
	Range	2.12–3.71	2.45–4.76	2.68–4.95	3.73–5.93	2.83–4.14

Note: items with ratings closer to 1 were considered more typical exemplars of the semantic category whereas items with ratings closer to 5 were considered more atypical exemplars of the category.

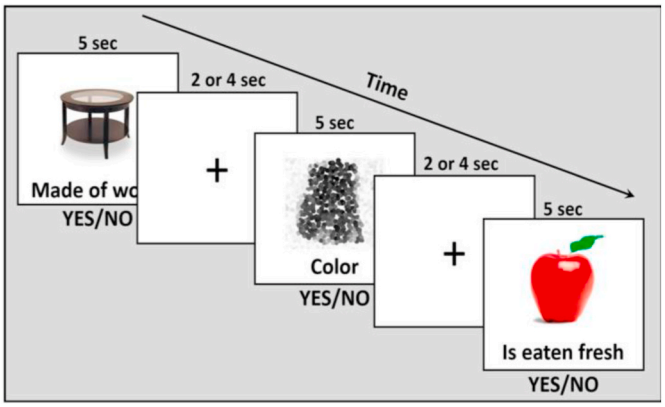

Fig. 2. Semantic feature verification task. Each trial was presented on the screen for 5 s, followed by a fixation cross for 2–4 s before the next trial appeared. Participants were asked to press the button to indicate whether the semantic feature (at the bottom of each trial) applied to each picture.

procedure. Reaction times and response accuracy were recorded for data analyses.

2.5. fMRI data acquisition

Participants were scanned at the Athinoula A. Martinos Center for Biomedical Imaging in Charlestown, MA on a 3T Siemens Trio Tim using a 20-channel head + neck coil. T1 images were acquired with TR = 2300 ms, TE = 2.91 ms, 176 sagittal slices, 1 × 1 × 1 mm voxels, 256 × 256 matrix, FOV = 256 mm, flip angle = 9°, fold-over direction = AP. Functional images were acquired via a gradient echo T2*-weighted EPI sequence, with TR = 2570 ms, TE = 30 ms, 40 axial slices, 3 mm slices interleaved with 2 × 2 × 3 mm voxels, 80 × 78 matrix, FOV = 220 × 220 mm, 40 axial, flip angle = 90°, parallel imaging with acceleration factor of 2.

2.6. fMRI preprocessing

For both groups, the MRI images were preprocessed following a standard pipeline in SPM12 (Ashburner et al., 2014), including slice timing with reference to the middle slice to account for differences in the timing of slice acquisition and realignment to correct for motion during scanning. Functional images were coregistered with the T1 structural scan, which was segmented into grey matter, white matter and cerebrospinal fluid based on the tissue probability maps in SPM12. Normalization of structural and functional images to Montreal Neurological Institute (MNI) space was then performed using 4th-degree b-spline interpolation. Finally, functional data were spatially smoothed using a 4-mm FWHM smoothing kernel for the purpose of univariate analysis (Meinzer et al., 2013). Another set of normalized but unsmoothed functional images was prepared for performing the searchlight MVPA (Kamitani and Sawahata, 2010).

A few additional steps were incorporated for patient data. Specifically, binarized lesion masks (in which lesioned voxels were deleted) for all PWA were manually drawn based on T1 images in MRIcron (Rorden and Brett, 2000). Binarized lesion masks and lesion maps (in which lesioned voxels were preserved) were included during preprocessing to improve coregistration and normalization (Brett et al., 2001). Normalized structural and functional data were visually compared to the template using the Check Reg function for SPM12, and images that were insufficiently aligned were manually corrected. The Artifact Detection Toolbox (ART) for SPM12 (Ashburner et al., 2014) was used to detect noise due to movement-related artifacts based on a linear motion threshold of 2 mm, rotational motion threshold of 0.5 radians, or global signal deviation of more than three standard deviations from the mean image intensity.

2.7. Data analysis

2.7.1. Lesion volume and percent of spared tissue

The anatomical ROIs were extracted from the AAL Atlas using the MarsBAR toolbox for SPM (Brett et al., 2002). Total lesion volume and the percentage of spared tissue in each anatomical ROI were calculated based on patients' normalized lesion maps. Specifically, any overlap between each patient's lesion map and the atlas-based left hemisphere ROIs was deleted, which created a set of ROIs comprising only spared tissue for each patient. The percentage of spared tissue in each ROI was then calculated using the volume of each of the spared tissue ROIs, divided by the total volume of the region from the AAL atlas, and multiplied by 100 (Sims et al., 2016). In PWA, the visual regions were spared as indicated by the percentage of spared tissues in the middle occipital gyrus (MOG; mean = 99.74 ± 0.57%), calcarine cortex (99.96 ± 0.19%), inferior occipital gyrus (IOG; mean = 100 ± 0%), and superior occipital gyrus (SOG; mean = 99.93 ± 0.25%).

2.7.2. Behavioral analysis

In order to examine participants' behavioral performance in the fMRI semantic feature verification task, mixed-effects models were performed using the *lmerTest* package (Kuznetsova et al., 2017) in R Studio Version 3.6.3 (Rstudio Team, 2016). Data were missing from run 2 of PWA19 and both runs of PWA18 and PWA20 due to technical issues of recording. Hence, these data were excluded from the behavioral analysis as these 0s could bias group comparisons and undermine mixed-effects models in PWA.

A generalized linear mixed-effects model for binomial data was conducted to determine the effect of semantic typicality on response accuracy (0 = inaccurate, 1 = accurate), and a linear mixed-effects model was conducted to determine the effect of semantic typicality on accurate reaction times. In both models, the fixed factors included semantic typicality (*typical, atypical*), group (healthy adults, PWA), and the typicality-by-group interaction term. Semantic category (*fruits, vegetables, clothing, birds, furniture*) was entered as a covariate. Random structure included a random intercept for subjects and a random slope for typicality. In order to estimate the fixed effects, sum-to-zero contrasts were coded for fixed factors (i.e., typicality, group, category), so that the mean of the dependent variable for a given level was compared to the overall mean of the dependent variable (i.e., main effect). Statistical

significance was set at $p < 0.05$.

2.7.3. Univariate fMRI analysis

For the first-level univariate analysis, the normalized and smoothed functional images for each individual were passed to a generalized linear modeling (GLM), which was used to obtain beta images associated with each condition (*typical, atypical*), and to test whether the results were similar or different from the searchlight analysis. Stimulus onsets and durations were convolved with the canonical hemodynamic response function (HRF) and its temporal derivative (Johnson et al., 2019). Conditions included *typical, atypical,* and *scrambled pictures*. Each condition was modeled separately for each run and both runs were concatenated within the GLM. Motion correction parameters that were obtained from realignment were included. Additionally, a grey matter mask was applied in the model to exclude the blood-oxygen-level-dependent (BOLD) signals in other anatomical segmentations such as white matter and cerebrospinal fluid (CSF). The main contrasts of interest were *typical* > *atypical* and *atypical* > *typical.*

A contrast image from the 1st-level analysis was then submitted to a 2nd-level univariate analysis (one-sample *t*-test) to examine differences of brain activation between typical and atypical conditions for each group of participants. The resulted *t*-maps were thresholded voxelwise at $p < 0.001$ (uncorrected) and then corrected for multiple comparisons using a cluster-level familywise error rate (FWE) correction at $p < 0.05$. Uncorrected results were reported if no clusters of voxels showed significance after correction.

2.7.4. Searchlight MVPA

In order to investigate which brain regions were sensitive to neural encoding of semantic typicality, a whole-brain searchlight analysis was performed (Kriegeskorte et al., 2006) using *The Decoding Toolbox* (TDT; Hebart et al., 2015) on the normalized but unsmoothed images in each group separately. TDT offers an interface with Statistical Parametric Mapping (SPM; http://www.fil.ion.ucl.ac.uk/spm/) in MATLAB (MathWorks, Inc., 2015). Beta values from the 1st-level univariate analysis were fed into the MVPA (Haynes et al., 2007; Mumford et al., 2012; Schrouff et al., 2013). Steps for performing the searchlight analysis are demonstrated in Fig. 3.

In the individual searchlight analysis, beta images for each condition (*typical, atypical*) in each run were first extracted from the 1st-level univariate analysis. A brain mask that was created during model estimation in the 1st-level univariate analysis was automatically used to reduce the searchlight space to voxels inside the brain. Next, a decoding searchlight analysis between the conditions *typical* and *atypical* was executed with a 9 mm radius, using a binary linear support vector machine (LSVM; Cortes and Vapnik, 1995) as a classifier (*LIBSVM* package in MATLAB; Chang and Lin, 2011) with a leave-one-run-out (LORO) cross-validation approach. That is, an LSVM classifier was trained with the data from one run used as the training set, and its performance was assessed on the data from the other run used as the testing set. The mean cross-validated accuracy was then stored at the central voxel in each searchlight sphere. This whole procedure was repeated for all voxels in the brain, yielding an accuracy map for each individual that included cross-validated accuracies ranging from −50 to 50 (0 represents the chance-level).

The above individual searchlight analysis was then repeated in each individual for a group analysis. The resulting classification accuracy maps for all participants were first spatially smoothed (post-processed) at 6 mm FWHM in SPM12 (Ashburner et al., 2014). Then, these smoothed accuracy maps were subjected to a 2nd-level mixed-effects analysis for each group separately using a one-sample *t*-test in SPM12. The resulting *t*-maps indicated statistical significance of the group-level classification accuracy in each voxel against zero (chance-level). These *t*-maps were thresholded voxelwise at $p < 0.001$ (uncorrected) and corrected for multiple comparisons using a cluster-level FWE correction at $p < 0.05$.

3. Results

3.1. Behavioral results on the fMRI task

Fig. 4 displays the mean response accuracy and reaction times for typical and atypical conditions across subjects in each group.

Results from the logistic mixed-effects model predicting response accuracy captured a significant main effect of typicality ($\beta = -0.12$, $|z| = 2.47$, SE = 0.05, $p < 0.05$), but no main effect of group ($p = 0.10$) or a group-by-typicality interaction effect ($p = 0.22$). This finding suggests that responses to atypical items were significantly less accurate than typical items across groups, but this typicality effect did not differ significantly between healthy adults (*typical:* 80.86 ± 27.89%; *atypical:* 77.37 ± 25.14%) and PWA (*typical:* 68.81 ± 19.90%; *atypical:* 68.03 ± 17.76%). There was, in addition, a main effect of category (*fruits:* $\beta = -0.70$, $|z| = 9.81$, SE = 0.07, $p < 0.01$; *furniture*: $\beta = 0.59$, $|z| = 4.37$, SE = 0.14, $p < 0.01$), indicating that responses to *fruits* were less accurate than the grand mean (i.e., average across groups or typicality conditions) and responses to *furniture* were more accurate than the grand mean. *Post-hoc* pairwise comparisons (tukey method) were performed using the *emmeans* package in R Studio Version 3.6.3. Findings showed that responses to *fruits* were less accurate than *birds* ($p < 0.01$), *clothing* ($p < 0.01$), *furniture* ($p < 0.01$), and *vegetables* ($p < 0.01$), whereas responses to *furniture* were more accurate than *clothing* ($p < 0.05$) and *vegetables* ($p < 0.05$).

The linear mixed-effects model for predicting accurate reaction times revealed a significant main effect of semantic typicality ($\beta = 36.29$, $|t| = 3.25$, SE = 11.18, $p < 0.01$), but no significant main effect of group ($p = 0.97$) or a group-by-typicality interaction effect ($p = 0.15$). This finding indicates that responses to atypical items were significantly slower than typical items across groups, but the typicality effect did not differ significantly between healthy adults (*typical:* 1680 ± 243 ms; *atypical:* 1743 ± 212 ms) and PWA (*typical:* 1672 ± 517 ms; *atypical:* 1707 ± 521 ms). Results also showed a significant main effect of category (*fruits:* $\beta = 132.93$, $|t| = 6.84$, SE = 19.44, $p < 0.01$), indicating that responses to *fruits* were slower than the grand mean. *Post-hoc* pairwise comparisons revealed that responses to *fruits* were slower than *birds* ($p < 0.01$),

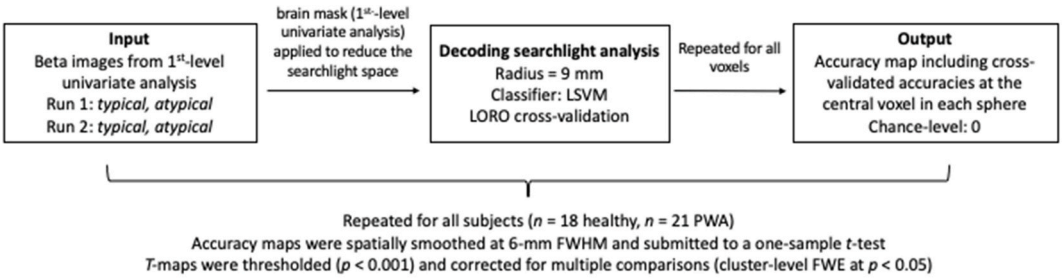

Fig. 3. Steps for performing the searchlight analysis. Upper section: three key components for performing the individual searchlight analysis. Lower section: group-level analysis.

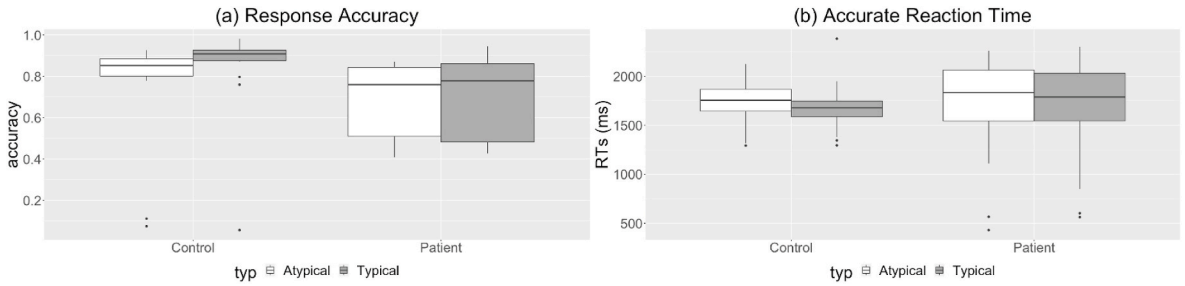

Fig. 4. Task performance in healthy individuals and PWA. Boxplots demonstrating the mean response accuracy in rates (a; 1.0 = 100%) and reaction times for accurate trials in milliseconds (b) across participants by condition in each group. Error bars: mean ± standard deviation.

clothing ($p < 0.01$), *furniture* ($p < 0.01$), and *vegetables* ($p < 0.01$).

3.2. Searchlight MVPA

Table 3 and Fig. 5 exhibit results of the group-level searchlight analysis in healthy adults and PWA. In the healthy group, significant above-chance searchlight classification between typical and atypical items was found in two clusters: left middle occipital gyrus (LMOG) extending into the left lingual gyrus, and right calcarine cortex extending into the right superior occipital gyrus (RSOG). In the patient group, no clusters of voxels showed significance after correction for multiple comparisons. At the uncorrected level (voxelwise at $p < 0.001$), we found neural classification in the right Rolandic operculum, left fusiform gyrus and right precuneus.

3.3. Relationship between task performance and neural classification

Although the searchlight MVPA did not reveal any significant results in PWA, a follow-up analysis was conducted to examine the association between the visual representation of semantic typicality and behavioral performance in our patients.

An ROI MVPA was first conducted to extract individual PWA's classification accuracy from the LMOG and right calcarine in PRoNTo 2.1 (Schrouff et al., 2013). Functional ROIs for the LMOG and right calcarine were extracted from healthy individuals based on the group-level classification results using the MarsBAR toolbox for SPM12 (Brett et al., 2002). Within each ROI, an MVPA was performed using a binary LSVM classifier with LORO cross-validation (see Appendix C for individual classification accuracy in each ROI).

Next, *Spearman's* rank correlations were conducted to examine the relationship between neural classification accuracy in each ROI and (1) the mean reaction times (RTs), (2) the mean accurate RTs, and (3) the mean percent accuracy across typical and atypical trials in the fMRI task, as well as assessment scores in the (4) PPT, which was administered to examine semantic association abilities. For correlational analysis (1)–(3), PWA18 and PWA20 were excluded and PWA19's behavioral performance was represented using data from run 1 due to their missing behavioral data in the fMRI task. P-values were then adjusted for multiple comparisons using the Benjamini-Hochberg procedure (FDR < 0.05). A significant positive association was found between the mean RTs across all typical and atypical trials and neural classification in the LMOG ($\rho = 0.57$, $p = 0.01$; Fig. 6). This correlation remained significant after p-values were adjusted ($p = 0.04$).

Table 3
Group-level searchlight results in healthy individuals and PWA.

Region	Cluster size	t-value	x	y	z
Healthy (cluster-level FWE correction at p < 0.05)					
L MOG	148	5.82*	−27	−84	6
L Lingual	148	5.23*	−15	−81	−6
R Calcarine	122	5.32*	18	−81	9
R SOG	122	5.08*	24	−84	15
PWA (uncorrected at p < 0.001)					
R Rolandic operculum	3	3.88	45	−27	21
L Fusiform	3	3.87	−33	−36	−24
R Precuneus	2	3.57	15	−63	21

L: Left, R: Right, MOG: middle occipital gyrus, SOG: superior occipital gyrus; x, y, and z correspond to peak MNI coordinates; *: FWE correction at $p < 0.05$.

3.4. Univariate fMRI analysis

Results in healthy adults showed a significant cluster of voxels in the right supramarginal gyrus (RSMG; $t = 5.71$, $k = 34$, MNI: x = 60, y = −42, z = 33) for *typical* > *atypical* (Fig. 7). Another cluster of voxels (uncorrected voxelwise at $p < 0.001$, cluster size $k \geq 10$) was found in the left cerebellum ($t = -5.92$, MNI: x = −21, y = −81, z = −21) for *atypical* > *typical*, but no significance was identified after multiple comparison correction. Results in PWA (uncorrected voxelwise at $p < 0.001$) showed activation in the right MOG ($t = 3.87$, MNI: x = 30, y = −84, z = 24) and left lingual gyrus ($t = 3.8$, MNI: x = −21, y = −84, z = −15) for *atypical* > *typical*, and in the right superior frontal gyrus ($t = 5.20$, MNI: x = 21, y = 6, z = 54), left cerebellum ($t = 3.88$, MNI: x = −12, y = −45, z = −24), and right supplementary motor area ($t = 3.59$, MNI: x = 12, y = 0, z = 54) for *typical* > *atypical*.

3.5. Post-hoc within-category univariate analysis

One potential difficulty with interpreting the afore-mentioned results is that the analyses were conducted for typical vs. atypical while collapsing across categories. Thus, to further assess if the effects of typical vs. atypical were maintained within specific categories, a univariate analysis was conducted to examine brain activation patterns for *typical* and *atypical* conditions within each category. The model structure was the same as the previous univariate analysis. In healthy adults, significant clusters of voxels (cluster-level FWE corrected at $p < 0.05$; Fig. 8a) were found for *atypical fruits* > *typical fruits* in the RSOG ($t = 8.97$, MNI: x = 18, y = −99, z = 15) extending into the right calcarine cortex ($t = 6.53$, MNI: x = 12, y = −99, z = 3), and in the LMOG ($t = 6.87$, MNI: x = −15, y = −102, z = 6) extending into the left calcarine cortex ($t = 6.16$, MNI: x = 12, y = −99, z = 3). No significant clusters were found for the other four categories after correction for multiple comparisons. In PWA, significant brain activation was identified for *atypical fruits* > *typical fruits* in the left lingual gyrus ($t = 5.62$; MNI: x = −3, y = −78, z = −3; cluster-level FWE corrected at $p < 0.05$; Fig. 8b). No significant results were found for the other four categories.

4. Discussion

The current study aimed to examine the processing of typical and atypical exemplars in both healthy individuals and PWA. Behavioral responses in the fMRI task showed that typical items were processed faster and more accurately than atypical items across both groups of participants. The searchlight MVPA across all categories demonstrated neural representation of semantic typicality in the visual cortex in

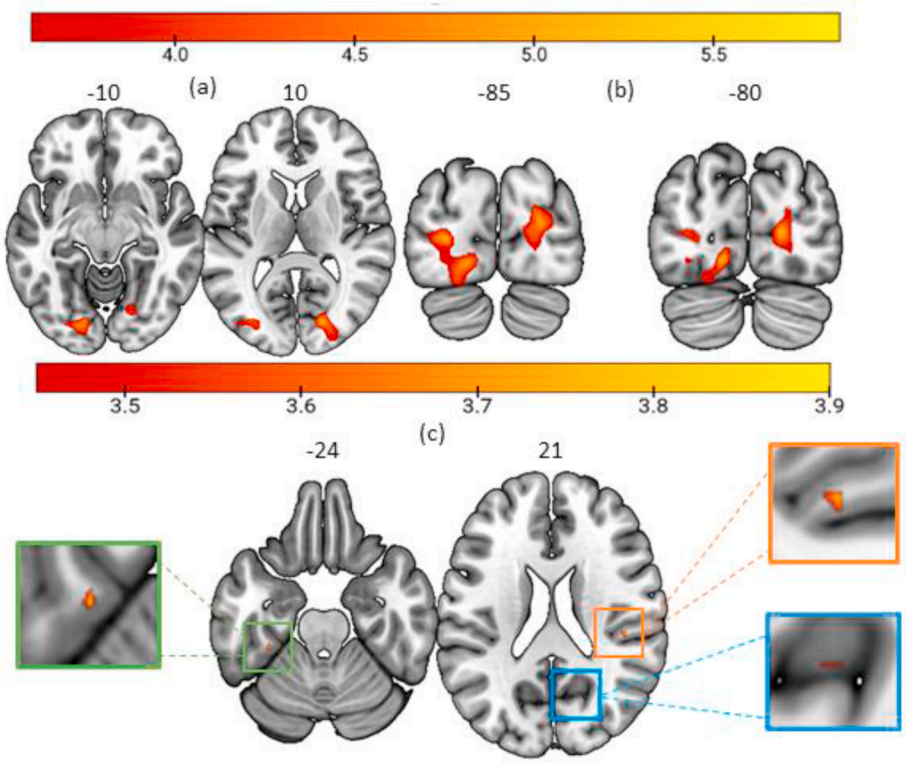

Fig. 5. Searchlight results in healthy individuals and PWA. Statistical significance for classification against chance-level in healthy participants (thresholded at $p < 0.001$, cluster-level FWE-corrected at $p < 0.05$), shown in axial (a) and coronal (b) views. Color bar indicates *t*-statistics (from 3.65 to 5.82), significant clusters were found in the LMOG and right calcarine cortex; Statistical significance for classification against chance-level in PWA (uncorrected at $p < 0.001$), shown in axial slices (c). Color bar indicates *t*-statistics (from 3.45 to 3.9), clusters were found in the left fusiform gyrus (green), right Rolandic operculum (orange) and right precuneus (blue). Figures are oriented in neurological convention. (For interpretation of the references to color in this figure legend, the reader is referred to the Web version of this article.)

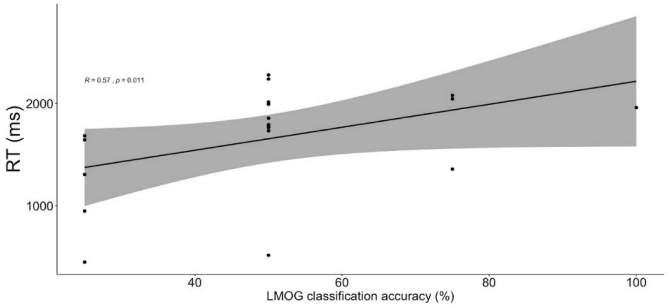

Fig. 6. Relationship between neural classification and fMRI task performance in PWA. Scatterplot depicting the relationship between neural classification in the LMOG and RTs across all typical and atypical trials in the fMRI task ($n = 19$ PWA). X-axis: neural classification accuracy (% accuracy); y-axis: mean reaction times (milliseconds).

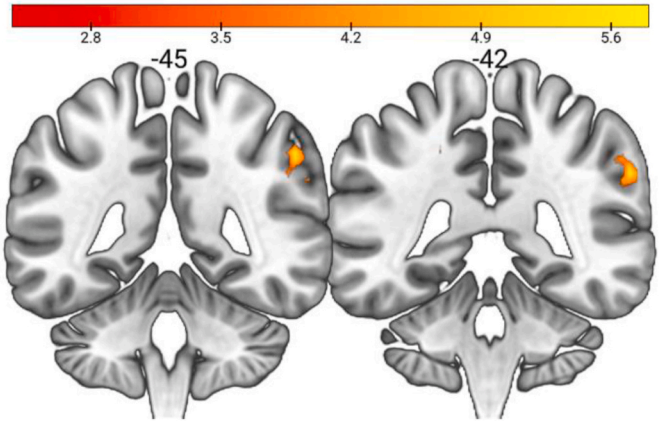

Fig. 7. Brain activation for *typical* > *atypical* revealed by the univariate analysis in healthy individuals. Coronal slices showing significant brain activation in the RSMG (cluster-level FWE correction at $p < 0.05$). No significant activation was found for *atypical* > *typical*. Images were displayed in neurological convention.

healthy individuals but did not reveal any significance in PWA. A follow-up correlational analysis in PWA showed a significant positive association between neural classification in the LMOG and response times in the fMRI task. At the univariate level when all categories were included, a significant cluster was found for *typical* > *atypical* in the RSMG in healthy individuals, but no significance was found for *atypical* > *typical* or for either contrast in PWA. However, when each category was analyzed separately, significant clusters of voxels were identified in the LMOG and RSOG for *atypical fruits* > *typical fruits* in healthy individuals, and another significant cluster was identified in the left lingual gyrus for the same contrast in PWA. Neural representation of typicality has been previously identified in visual (i.e., right LOC; Iordan et al., 2016) and temporal regions (i.e., right temporal fusiform and medial temporal lobes; Davis and Poldrack, 2014) in healthy young individuals. The present study differed from these previous studies in that we included both older healthy adults and patients with post-stroke aphasia. In what follows, we discuss the main behavioral and neuroimaging findings across the two groups addressed in this study.

4.1. Behavioral typicality effect

The current study found a main effect of typicality. Specifically, responses to typical items were faster and more accurate than atypical items across healthy adults and PWA. These findings are consistent with previous behavioral studies examining the effects of typicality in both healthy individuals (Rosch et al., 1976; Hampton, 1995) and PWA (Kiran and Thompson, 2003; Kiran et al., 2007; Sandberg et al., 2012), suggesting that atypical exemplars of a category are more difficult to process than typical exemplars. However as suggested by Roger et al. (2015), the typicality effect may be governed by specific tasks. In their study, patients with SA showed significant typicality effects in picture

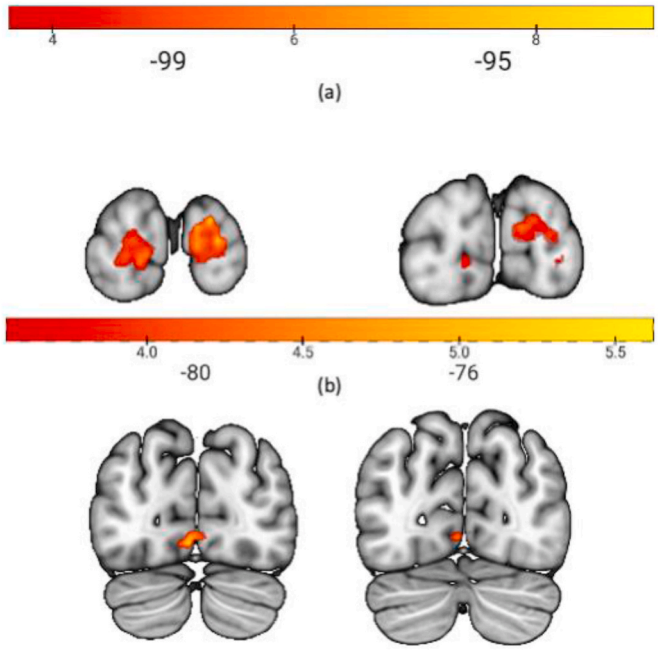

Fig. 8. *Atypical fruits* > *Typical fruits* in (a) healthy adults and (b) PWA. (a) Significant clusters in the RSOG extending into the right calcarine cortex, and in the LMOG extending into the left calcarine cortex; (b) significant cluster in the left lingual gyrus. Color bars indicate *t*-statistic (cluster-level FWE corrected at $p < 0.05$). Figure is oriented in neurological convention (left is on the left). (For interpretation of the references to color in this figure legend, the reader is referred to the Web version of this article.)

sorting and word-picture matching tasks, but not in the picture naming task. Their findings were interpreted within the context of semantic control. Since the semantic impairment in SA can arise from damage to the control network (i.e., prefrontal and/or temporo-parietal regions), the processing of typicality might be affected if the tasks require a greater degree of control. Nevertheless, we think task-dependency does not affect our findings as our fMRI task did not require semantic control such as inhibiting specific feature properties or selecting a target item among other strongly competing distractors.

The regression analyses of response times and accuracy did not reveal a main effect of group or the group-by-typicality interaction. Previous studies investigating semantic typicality found significantly lower accuracy and longer RTs in PWA than healthy adults (Kiran and Thompson, 2003; Sandberg et al., 2012). A main difference between these previous studies and the current study is that they compared patients with different types of aphasia or levels of semantic impairment. Hence, including PWA of different aphasia types and severity in a single group might have led to an insignificant group effect or an interaction effect in our study. Note that the goal of this study was not to examine semantic typicality in different age groups or patients with various aphasia severities. Another explanation to this finding is that two healthy adults (HP2 and HP7) scored below chance (50% accuracy) in the fMRI task, which might also have resulted in an insignificant between-group difference.

Behavioral results further showed an effect of category, in which responses to *fruits* were slower and less accurate than the other categories and responses to *furniture* were more accurate than *fruits*, *clothing*, and *vegetables*. This category-specific effect was not initially hypothesized. We think this finding could be due to a relatively high overall familiarity of *furniture* and a low overall familiarity of *fruits*, which is a potential factor that might have affected the processing of typicality (Folstein and Dieciuc, 2019; Malt and Smith, 1982).

4.2. Neural correlates of semantic typicality in healthy adults

In order to identify the neural correlates of typicality, an MVPA was conducted in this study to detect different brain activation patterns between typical and atypical items (Kriegeskorte et al., 2006). Results in healthy adults revealed two neural clusters in the visual cortex with above-chance classification accuracy after correction for multiple comparisons (i.e., LMOG and right calcarine cortex). These findings partially support our hypothesis, which predicted distinct patterns of activation between typical and atypical exemplars in both visual and temporal regions. The univariate analysis in healthy adults revealed a significant cluster in the RSMG that indicated greater activation for *typical* > *atypical*. However, the distinction between typical and atypical exemplars in the visual cortex could have been affected by other factors than typicality itself. Given that a category effect was found in the behavioral data, it is possible that we inadvertently compared typical birds with atypical clothing and the difference emerged from a purely visual complexity aspect without capturing exemplar typicality effects. For this reason, we further examined the typicality effect for each category and found a significant typicality effect for fruits in regions that were consistent with the MVPA (i.e., LMOG and RSOG). Other categories did not show these findings likely because of lower sample sizes. These results suggest that MVPA allows for the capture of subtle neural differences in access and representation of semantic typicality by taking into account the relationships across voxels, whereas univariate analysis cannot (Haxby et al., 2001; Norman et al., 2006).

Our findings in the visual cortex are consistent with previous neuroimaging studies examining the typicality effect in healthy individuals (Davis and Poldrack, 2014; Iordan et al., 2016). Although the findings are not in the same visual regions as identified in previous studies (i.e., LOC in the Iordan study), these results support the hypothesis that neural representation of semantic typicality is built by the visual system at an intermediate processing stage, rather than being directly reflected in the stimulus input (Iordan et al., 2016). The LMOG and calcarine cortex have both been associated with visual semantic processing of different categories (Martin et al., 1996; Tyler et al., 2003), suggesting that these regions play an important role in processing the internal structure of categories.

The distinction between typical and atypical items in the visual cortex might also be attributed to other psycholinguistic and perceptual factors, such as familiarity (Boster, 1988) and lower visual features (e.g., color relatedness; Huth et al., 2012). Even though our study was not aimed to investigate these potential factors, we have attempted to further clarify whether our picture stimuli differed in color-related features between typical and atypical exemplars. Color features were extracted using the rgb2hsv function in R Studio ("grDevices" package; Rstudio Team, 2016), which provided values of hue, saturation, vibrancy, contrast, and clarity. For each of these features, a simple linear regression was conducted to estimate the effect of typicality (i.e., typical, atypical) across all the stimuli. We did not find any significance between typical and atypical stimuli, suggesting that the pictures were unlikely confounded by color-related parameters. One could argue whether the relations among the stimuli are correlated to the relations among their neural representations. These questions are better examined using other approaches such as the representational similarity analysis (RSA; Kriegeskorte et al., 2008). The current experimental design, however, was not well suited to compute a dissimilarity matrix ideal to complete an RSA, hence we were unable to implement this analysis to examine these issues. Future research is needed to tease apart potential factors, including familiarity of the objects, motion-related features of the picture stimuli, and lexical interference of the features that may differentially affect the typicality representation in the brain.

Results from our searchlight MVPA surprisingly did not capture above-chance classification in any temporal regions in healthy adults, which is contrary to our hypothesis. Comparing to one previous study that found typicality representation in the temporal cortex (Davis and

Poldrack, 2014), our study had relatively fewer trials and runs that might have led to a diminished effect in the temporal cortex. Alternatively, it is possible that semantic feature verification for typical and atypical examples is similar in a way that does not elicit temporal activation.

Nevertheless, the neural correlates of typicality in healthy adults can be explained by theoretical models. One explanation of the distinction between typical and atypical exemplars that appeared in the visual but not the temporal cortex is based on the prototype theory, which assumes that the degree of shared features could be different between typical and atypical exemplars (Rosch and Mervis, 1975). Note that some of the features required perceptual processing (i.e., apple: is round; parrot: has feathers) whereas other features required functional/semantic knowledge (e.g., blouse: worn by women; washing machine: needs power to work) about the example in question. The current results of a typicality effect in the visual cortex (i.e., MOG) but not in the temporal lobe (i.e., MTG) even in the healthy adults would suggest that such type of featural verification may be occurring in the visual cortex. The present results can likely be better explained by the exemplar theory (Nosofsky and Palmeri, 1997; Nosofsky and Zaki, 2002), which posits that categories are represented based on the stored exemplars in memory, and that typicality is conceptualized as how similar each item is to the stored exemplars in memory. Here, the typicality effect identified in the visual cortex suggests that these regions may participate in visual and semantic processing as participants might have completed the featural verification task by comparing features for specific examples as stored memory representations rather than as a set of distributed featural representations.

4.3. Neural correlates of semantic typicality in PWA

In PWA, different patterns of activation were identified for the processing of typical and atypical exemplars. Specifically, the uncorrected results from the searchlight MVPA showed three clusters of voxels in the right Rolandic operculum, left fusiform gyrus and right precuneus. These regions did not show significance after correction for multiple comparisons, so it is difficult to draw conclusions about the roles of these regions. However, a follow-up correlational analysis captured a significant positive association between reaction times in the fMRI task and neural classification in the LMOG, suggesting that the typicality effect was more likely identified in the visual cortex in patients who spent longer versus shorter time verifying semantic features. At the univariate level, no significance was identified for *typical* > *atypical* or *atypical* > *typical*. When examining the activation patterns within each category, a significant cluster was found in the left lingual gyrus for *atypical fruits* > *typical fruits*. Even though the results from MVPA did not capture any significance, the brain-behavioral correlation and the within-group univariate analysis for fruits suggest that neural representation of semantic typicality might still be modulated by visual regions in PWA, yet to a much lesser extent than healthy individuals.

While there was no temporal activation corresponding to the typicality effect in healthy adults, in PWA, we were unable to examine potential activation since all our participants had damage in the temporal lobe. One possibility for the results in PWA is that temporal lesions may cause damage to the functional connectivity between temporal and visual regions that affects the processing of all typical and atypical items. Numerous neuroimaging studies have indicated the importance of functional connection in cognitive processes as behavioral deficits may emerge from any damage in the regions of a network (Catani and Ffytche, 2005; Toba et al., 2020). Hence, although the visual cortex was spared in our patients, brain damage in any part of the temporal lobe could result in functional deficits in semantic processing of typicality. However, this tentative account should be examined in future studies using other neuroimaging techniques such as dynamic causal modelling to examine the functional interactions between the visual and temporal lobes. As such, in this study, it is difficult to draw any conclusions about the role of the temporal lobe in the processing of typicality for PWA.

4.4. Limitations and future directions

One limitation of the current study is a relatively small sample size of task stimuli, which could lead to cross-validation failure with large error in multi-voxel pattern analysis, as suggested by previous studies (Varoquaux, 2018). Additionally, the neural representation of typicality can be associated with other psycholinguistic factors, such as familiarity, frequency, animacy, etc. Although the current study was not aimed to examine the effects of these factors, future studies should utilize approaches such as RSA (Kriegeskorte et al., 2008) to establish the correspondence between the relations among stimuli and the relations among their brain activation patterns in order to tease apart these potential variables. This approach would require more samples of task trials to examine factors that may influence the neural distinction between typical and atypical stimuli in the visual cortex. Another direction is to include subgroups of PWA based on whether there is damage to the temporal lobe or not in order to understand the role of the temporal lobe in typicality processing. As pointed out by Price et al. (2006), activation may not be detected in patients if they are grouped on the basis of similar lesion patterns as this could bias the interpretation of patient-specific responses. Furthermore, the typicality effect could also be affected by the impaired semantic control ability in PWA, as suggested by Rogers et al. (2015). So, it would be informative if future studies could gather information about semantic control in order to examine its role in the processing of items or tasks that require semantic control.

5. Conclusion

The current study aimed to identify brain regions that show differential neural activation patterns between typical and atypical exemplars in both healthy adults and PWA. The behavioral results showed that responses to typical items were faster and more accurate than atypical items. A searchlight MVPA revealed that semantic typicality was represented in the visual cortex in healthy adults, whereas results were not significant in PWA. A follow-up analysis in PWA showed a strong association between neural classification in the LMOG and reaction times in the fMRI task. When the typicality effect was examined for each category at the univariate level, significance was identified for fruits in the visual cortex in both healthy individuals and PWA. These findings suggest that typicality was modulated in the visual cortex in healthy individuals, but to a lesser extent in the same region in PWA. Future studies can include patients on the basis of damage to the temporal lobe and incorporate other neuroimaging techniques to establish the roles of temporal and visual regions in typicality processing.

Credit statement

Ran Li: Conceptualization, Methodology, Software, Formal analysis, Writing – original draft, Writing – review & editing, Visualization. Swathi Kiran: Conceptualization, Methodology, Investigation, Resources, Writing – review & editing, Supervision, Funding acquisition. Tyler Perrachione: Conceptualization, Methodology, Formal analysis; Jason Tourville: Conceptualization, Methodology, Formal analysis.

Funding

This work was supported by National Institute on Deafness and Other Communication Disorders of the National Institutes of Health (USA) under grant 1P50DC012283. The authors report no conflict of interest. Ran Li was supported by grant from the NIH/NIDCD (1U01DC014922). Jason Tourville was supported by grants from the NIH/NIDCD (R01 DC002852 and R01 DC007683). Swathi Kiran is a scientific consultant for The Learning Corporation (FKA Constant Therapy) but there is no

scientific overlap with the work in this project.

Acknowledgements

The authors extend their gratitude to all of the individuals who participated in this study. We also thank previous members from the Aphasia Research Laboratory at Boston University for their assistance in data collection, and Natalie Gilmore, Maria Varkanitsa, Claudia Peñaloza, Michael Scimeca and Claire Cordella for providing feedback to this article.

Appendix A. Sample stimuli from five semantic categories used in the fMRI task

Animate					
Vegetables		Birds		Fruits	
Typ	Atyp	Typ	Atyp	Typ	Atyp
squash	parsley	dove	penguin	grapefruit	plantain
corn	okra	lark	duck	orange	date
turnip	rutabaga	sparrow	heron	strawberry	pomelo
artichoke	dill	pigeon	peacock	plum	huckleberry
radish	alfalfa	oriole	parrot	apple	boysenberry
onion	chives	canary	stork	banana	crabapple
tomato	seaweed	owl	emu	lemon	lychee
potato	endives	raven	goose	grape	fig
celery	yam	chicken	condor	blueberry	raisin
carrot	scallion	quail	albatross	cranberry	papaya
Inanimate					
Furniture				Clothing	
Typ	Atyp			Typ	Atyp
chair	piano			dress	cape
bed	stove			tuxedo	apron
bookcase	furnace			khakis	cummerbund
mirror	sink			skirt	earmuffs
dresser	hammock			sock	overalls
footstool	refrigerator			jacket	raincoat
loveseat	rug			robe	pantyhose
desk	trunk			blouse	tie
bench	blinds			coat	vest
table	curtains			jeans	suspenders

Typ: Typical; Atyp: Atypical.

Appendix B. Sample semantic features used in the fMRI task

	Category				
Feature Type	Fruits	Vegetables	Birds	Clothing	Furniture
Defining	ripens	edible	has wings	has sizes	sits on the floor
Characteristic	is sweet	is green	colorful	has buttons	made of metal
Unrelated	has yellow flesh	is juicy	is large	wool	has shelves
Non-category	swims	is knitted	spicy	has lights	is loud

Appendix C. Individual PWA's classification accuracy in the LMOG and right calcarine

Patient ID	**LMOG (%)**	**Right calcarine (%)**
PWA1	25	50
PWA2	50	50
PWA3	75	50
PWA4	100	50
PWA5	50	25
PWA6	75	50
PWA7	50	50
PWA8	50	25
PWA9	25	50
PWA10	50	50
PWA11	25	50
PWA12	75	50
PWA13	25	75
PWA14	50	25
PWA15	50	50
PWA16	50	50

(*continued on next page*)

(*continued*)

Patient ID	LMOG (%)	Right calcarine (%)
PWA17	50	50
PWA18[a]	50	25
PWA19[b]	25	25
PWA20[a]	50	50
PWA21	50	50
Mean	50	45.24
SD	19.36	12.79

[a] These two patients were excluded from the correlational analysis (1)–(3) due to incomplete behavioral data.

[b] This patient's fMRI task performance was represented with data from run 1 due to incomplete behavioral data. PWA: patients with aphasia.

References

Ashburner, J., Barnes, G., Chen, C., Daunizeau, J., Flandin, G., Friston, K., et al., 2014. SPM12 Manual. Wellcome Trust Centre for Neuroimaging, London, UK, p. 2464.

Bandettini, P.A., Cox, R.W., 2000. Event-related fMRI contrast when using constant interstimulus interval: theory and experiment. Magn. Reson. Med.: An Official Journal of the International Society for Magnetic Resonance in Medicine 43 (4), 540–548 https://doi.org/10.1002/(SICI)1522-2594(200004)43:4<540::AID-MRM8>3.0.CO;2-R.

Binder, J.R., Desai, R.H., 2011. The neurobiology of semantic memory. Trends Cognit. Sci. 15 (11), 527–536. https://doi.org/10.1016/j.tics.2011.10.001.

Binder, J.R., Desai, R.H., Graves, W.W., Conant, L.L., 2009. Where is the semantic system? A critical review and meta-analysis of 120 functional neuroimaging studies. Cerebr. Cortex 19 (12), 2767–2796. https://doi.org/10.1093/cercor/bhp055.

Boster, J.S., 1988. Natural sources of internal category structure: typicality, familiarity, and similarity of birds. Mem. Cognit. 16 (3), 258–270. https://doi.org/10.3758/BF03197759.

Brett, M., Anton, J.L., Valabregue, R., Poline, J.B., 2002, June. Region of interest analysis using an SPM toolbox. In: 8th International Conference on Functional Mapping of the Human Brain, vol. 16, p. 497. No. 2.

Brett, M., Leff, A.P., Rorden, C., Ashburner, J., 2001. Spatial normalization of brain images with focal lesions using cost function masking. Neuroimage 14 (2), 486–500. https://doi.org/10.1006/nimg.2001.0845.

Catani, M., Ffytche, D.H., 2005. The rises and falls of disconnection syndromes. Brain 128 (10), 2224–2239. https://doi.org/10.1093/brain/awh622.

Chang, C.C., Lin, C.J., 2011. LIBSVM: a library for support vector machines. ACM transactions on intelligent systems and technology (TIST) 2 (3), 1–27.

Coltheart, M., 1981. The mrc psycholinguistic database. The Quarterly Journal of Experimental Psychology Section A 33 (4), 497–505. https://doi.org/10.1080/14640748108400805.

Cortes, C., Vapnik, V., 1995. Support-vector networks. Mach. Learn. 20 (3), 273–297. https://doi.org/10.1007/BF00994018.

Davis, T., Poldrack, R.A., 2014. Quantifying the internal structure of categories using a neural typicality measure. Cerebr. Cortex 24 (7), 1720–1737. https://doi.org/10.1093/cercor/bht014.

Etzel, J., Zacks, J., Braver, T., 2013. Searchlight analysis: promise, pitfalls, and potential. Neuroimage 78, 261–269. https://doi.org/10.1016/j.neuroimage.2013.03.041.

Folstein, J.R., Dieciuc, M.A., 2019. The cognitive neuroscience of stable and flexible semantic typicality. Front. Psychol. 10, 1265 https://doi.org/10.3389/fpsyg.2019.01265.

Gainotti, G., 2000. What the locus of brain lesion tells us about the nature of the cognitive defect underlying category-specific disorders: a review. Cortex 36 (4), 539–559. https://doi.org/10.1016/S0010-9452(08)70537-9.

Gilmore, N., Meier, E.L., Johnson, J.P., Kiran, S., 2020. Typicality-based semantic treatment for anomia results in multiple levels of generalisation. Neuropsychol. Rehabil. 30 (5), 802–828. https://doi.org/10.1080/09602011.2018.1499533.

Hampton, J.A., 1979. Polymorphous concepts in semantic memory. J. Verb. Learn. Verb. Behav. 18 (4), 441–461. https://doi.org/10.1016/S0022-5371(79)90246-9.

Hampton, J.A., 1995. Testing the prototype theory of concepts. J. Mem. Lang. 35 (5), 686–708. https://doi.org/10.1006/jmla.1995.1031.

Haxby, J.V., Gobbini, M.I., Furey, M.L., Ishai, A., Schouten, J.L., Pietrini, P., 2001. Distrubuted and overlapping representations of face and objects in ventral temporal cortex. Science 293 (5539), 2425–2430. https://doi.org/10.1126/science.1063736.

Haynes, J.D., Sakai, K., Rees, G., Gilbert, S., Frith, C., Passingham, R.E., 2007. Reading Hidden intentions in the human brain. Curr. Biol. 17 (4), 323–328. https://doi.org/10.1016/j.cub.2006.11.072.

Hebart, M.N., Görgen, K., Haynes, J.D., 2015. The Decoding Toolbox (TDT): a versatile software package for multivariate analyses of functional imaging data. Front. Neuroinf. 8, 88. https://doi.org/10.3389/fninf.2014.00088.

Hillis, A.E., Caramazza, A., 1991. Category-specific naming and comprehension impairment: a double dissociation. Brain 114 (5), 2081–2094. https://doi.org/10.1093/brain/114.5.2081.

Howard, D., Patterson, K., 1992. The Pyramids and Palm Trees Test: A Test of Semantic Access from Words and Pictures. Pearson Assessment.

Huth, A.G., Nishimoto, S., Vu, A.T., Gallant, J.L., 2012. A continuous semantic space describes the representation of thousands of object and action categories across the human brain. Neuron 76 (6), 1210–1224. https://doi.org/10.1016/j.neuron.2012.10.014.

Iordan, M.C., Greene, M.R., Beck, D.M., Fei-Fei, L., 2016. Typicality sharpens category representations in object-selective cortex. Neuroimage 134, 170–179. https://doi.org/10.1016/j.neuroimage.2016.04.012.

Johnson, J.P., Meier, E.L., Pan, Y., Kiran, S., 2019. Treatment-related changes in neural activation vary according to treatment response and extent of spared tissue in patients with chronic aphasia. Cortex 121, 147–168. https://doi.org/10.1016/j.cortex.2019.08.016.

Kamitani, Y., Sawahata, Y., 2010. Spatial smoothing hurts localization but not information: pitfalls for brain mappers. Neuroimage 49 (3), 1949–1952. https://doi.org/10.1016/j.neuroimage.2009.06.040.

Kaplan, E., Goodglass, H., Weintraub, S., 2001. Boston Naming Test. Pro-.

Kay, J., Lesser, R., Coltheart, M., 1996. Psycholinguistic assessments of language processing in aphasia (PALPA): an introduction. Aphasiology 10 (2), 159–180.

Kertesz, A., 2007. Western Aphasia Battery-Revised (WAB-R). Pearson.

Kiran, S., Thompson, C.K., 2003. Effect of typicality on online category verification of animate category exemplars in aphasia. Brain Lang. 85 (3), 441–450.

Kiran, S., 2007. Complexity in the treatment of naming deficits. Am. J. Speech Lang. Pathol 16 (1), 18–29.

Kiran, S., Ntourou, K., Eubank, M., 2007. The effect of typicality on online category verification of inanimate category exemplars in aphasia. Aphasiology 21 (9), 844–866.

Kriegeskorte, N., Goebel, R., Bandettini, P., 2006. Information-based functional brain mapping. Proc. Natl. Acad. Sci. Unit. States Am. 103 (10), 3863–3868. https://doi.org/10.1073/pnas.0600244103.

Kriegeskorte, N., Mur, M., Bandettini, P.A., 2008. Representational similarity analysis-connecting the branches of systems neuroscience. Front. Syst. Neurosci. 2, 4. https://doi.org/10.3389/neuro.06.004.2008.

Kuznetsova, A., Brockhoff, P.B., Christensen, R.H.B., 2017. lmerTest package: tests in linear mixed effects models. J. Stat. Software 82 (13). https://doi.org/10.18637/jss.v082.i13.

Lambon Ralph, M.A.L., Jefferies, E., Patterson, K., Rogers, T.T., 2016. The neural and computational bases of semantic cognition. Nat. Rev. Neurosci. 18 (1), 42–55. https://doi.org/10.1038/nrn.2016.150.

Larochelle, S., Pineau, H., 1994. Determinants of response times in the semantic verification task. J. Mem. Lang. 33 (6), 796–823. https://doi.org/10.1006/jmla.1994.1038.

Mahmoudi, A., Takerkart, S., Regragui, F., Boussaoud, D., Brovelli, A., 2012. Multivoxel pattern analysis for FMRI data: a review. Computational and mathematical methods in medicine 1–14. https://doi.org/10.1155/2012/961257, 2012.

Malt, B.C., Smith, E.E., 1982. The role of familiarity in determining typicality. Mem. Cognit. 10 (1), 69–75. https://doi.org/10.3758/BF03197627.

Martin, A., Wiggs, C.L., Ungerleider, L.G., Haxby, J.V., 1996. Neural correlates of category-specific knowledge. Nature 379 (6566), 649–652. https://doi.org/10.1038/379649a0.

MathWorks Inc, 2005. MATLAB: the language of technical computing. In: Getting Started with MATLAB, Version 7, vol. 1. MathWorks, Incorporated.

Meier, E.L., Lo, M., Kiran, S., 2016. Understanding semantic and phonological processing deficits in adults with aphasia: effects of category and typicality. Aphasiology 30 (6), 719–749.

Meinzer, M., Beeson, P.M., Cappa, S., Crinion, J., Kiran, S., Saur, D., et al., 2013. Neuroimaging in aphasia treatment research: consensus and practical guidelines for data analysis. Neuroimage 73, 215–224. https://doi.org/10.1016/j.neuroimage.2012.02.058.

Mumford, J.A., Turner, B.O., Ashby, F.G., Poldrack, R.A., 2012. Deconvolving BOLD activation in event-related designs for multivoxel pattern classification analyses. Neuroimage 59 (3), 2636–2643. https://doi.org/10.1016/j.neuroimage.2011.08.076.

Norman, K.A., Polyn, S.M., Detre, G.J., Haxby, J.V., 2006. Beyond mind-reading: multi-voxel pattern analysis of fMRI data. Trends Cognit. Sci. 10 (9), 424–430. https://doi.org/10.1016/j.tics.2006.07.005.

Nosofsky, R.M., 1988. Exemplar-based accounts of relations between classification, recognition, and typicality. J. Exp. Psychol. Learn. Mem. Cognit. 14 (4), 700–708. https://doi.org/10.1037/0278-7393.14.4.700.

Nosofsky, R.M., Palmeri, T.J., 1997. An exemplar-based random walk model of speeded classification. Psychol. Rev. 104 (2), 266–300. https://doi.org/10.1037/0033-295X.104.2.266.

Nosofsky, R.M., Zaki, S.R., 2002. Exemplar and prototype models revisited: response strategies, selective attention, and stimulus generalization. J. Exp. Psychol. Learn. Mem. Cognit. 28 (5), 924–940. https://doi.org/10.1037/0278-7393.28.5.924.

Patterson, K., Nestor, P.J., Rogers, T.T., 2007. Where do you know what you know? The representation of semantic knowledge in the human brain. Nat. Rev. Neurosci. 8 (12), 976–987. https://doi.org/10.1038/nrn2277.

Price, C.J., Crinion, J., Friston, K.J., 2006. Design and analysis of fMRI studies with neurologically impaired patients. J. Magn. Reson. Imag. 23 (6), 816–826. https://doi.org/10.1002/jmri.20580.

Rogers, T.T., Patterson, K., Jefferies, E., Lambon Ralph, M.A., 2015. Disorders of representation and control in semantic cognition: effects of familiarity, typicality, and specificity. Neuropsychologia 76, 220–239. https://doi.org/10.1016/j.neuropsychologia.2015.04.015.

Rorden, C., Brett, M., 2000. Stereotaxic display of brain lesions. Behav. Neurol. 12 (4), 191–200. https://doi.org/10.1155/2000/421719.

Rosch, E., 1975. Cognitive representations of semantic categories. J. Exp. Psychol. Gen. 104 (3), 192–233. https://doi.org/10.1037/0096-3445.104.3.192.

Rosch, E., Mervis, C.B., 1975. Family resemblances: studies in the internal structure of categories. Cognit. Psychol. 7 (4), 573–605. https://doi.org/10.1016/0010-0285(75)90024-9.

Rosch, E., Simpson, C., Miller, R.S., 1976. Structural bases of typicality effects. J. Exp. Psychol. Hum. Percept. Perform. 2 (4), 491–502. https://doi.org/10.1037/0096-1523.2.4.491.

Rouder, J.N., Ratcliff, R., 2006. Comparing exemplar- and rule- based theories of categorization. Curr. Dir. Psychol. Sci. 15 (1), 9–13. https://doi.org/10.1111/j.0963-7214.2006.00397.x.

Rstudio Team, 2016. RStudio. Integrated development for R. RStudio, Inc., Boston MA. RStudio https://doi.org/10.1007/978-3-642-20966-6.

Sandberg, C., Gray, T., Kiran, S., 2020. Development of a free online interactive naming therapy for bilingual aphasia. Am. J. Speech Lang. Pathol 29 (1), 20–29. https://doi.org/10.1044/2019_AJSLP-19-0035.

Sandberg, C., Sebastian, R., Kiran, S., 2012. Typicality mediates performance during category verification in both ad-hoc and well-defined categories. J. Commun. Disord. 45 (2), 69–83. https://doi.org/10.1016/j.jcomdis.2011.12.004.

Schneider, W., Eschman, A., Zuccolotto, A., 2002. E-prime: User's Guide. Reference Guide. Getting Started Guide. Psychology Software Tools, Incorporated.

Schrouff, J., Rosa, M.J., Rondina, J.M., Marquand, A.F., Chu, C., Ashburner, J., et al., 2013. PRoNTo: pattern recognition for neuroimaging toolbox. Neuroinformatics 11 (3), 319–337. https://doi.org/10.1007/s12021-013-9178-1.

Sims, J.A., Kapse, K., Glynn, P., Sandberg, C., Tripodis, Y., Kiran, S., 2016. The relationships between the amount of spared tissue, percent signal change, and accuracy in semantic processing in aphasia. Neuropsychologia 84, 113–126. https://doi.org/10.1016/j.neuropsychologia.2015.10.019.

Toba, M.N., Godefroy, O., Rushmore, R.J., Zavaglia, M., Maatoug, R., Hilgetag, C.C., Valero-Cabré, A., 2020. Revisiting 'brain modes' in a new computational era: approaches for the characterization of brain-behavioural associations. Brain 143 (4), 1088–1098. https://doi.org/10.1093/brain/awz343.

Tyler, L.K., Moss, H.E., 1998. Going, going, gone ... ? Implicit and explicit tests of conceptual knowledge in a longitudinal study of semantic dementia. Neuropsychologia 36 (12), 1313–1323. https://doi.org/10.1016/S0028-3932(98)00029-3.

Tyler, L.K., Bright, P., Dick, E., Tavares, P., Pilgrim, L., Fletcher, P., et al., 2003. Do semantic categories activate distinct cortical regions? Evidence for a distributed neural semantic system. Cogn. Neuropsychol. 20 (3–6), 541–559.

Tyler, L.K., Moss, H.E., Durrant-Peatfield, M.R., Levy, J.P., 2000. Conceptual structure and the structure of concepts: a distributed account of category-specific deficits. Brain Lang. 75 (2), 195–231. https://doi.org/10.1006/brln.2000.2353.

Van der Wouden, T., 1990. Celex: building a multifunctional polytheoretical lexical data base. Proceedings of BudaLex 88, 363–373.

Varoquaux, G., 2018. Cross-validation failure: small sample sizes lead to large error bars. Neuroimage 180, 68–77. https://doi.org/10.1016/j.neuroimage.2017.06.061.